[22] R. A. Sammut and C. Pask, "Simplified numerical analysis of optical fibers and planar waveguides," *Electron. Lett.*, vol. 17, pp. 105-106, Feb. 1981.
[23] P. L. Francois, I. Sasaki, and M. J. Adams, "Practical three-dimensional profiling of optical fiber preforms," *IEEE J. Quantum Electron.*, vol. QE-18, pp. 524-535, Apr. 1982.
[24] D. N. Payne, A. J. Barlow, and J. J. Ramskov-Hansen, "Development of low- and high-birefringence optical fibers," *IEEE J. Quantum Electron.*, vol. QE-18, pp. 477-488, Apr. 1982.

Pierre-Luc Francois, for a photograph and biography, see p. 380 of the April 1982 issue of this TRANSACTIONS.

Single-Mode Fiber OTDR: Experiment and Theory

DAN L. PHILEN, IAN A. WHITE, JANE F. KUHL, AND STEPHEN C. METTLER

Abstract—**An OTDR measurement technique with an end detection dynamic range of 63 dB is described for use with single-mode fibers. A theoretical analysis of single-mode fiber backscattering is presented which predicts loss penalties in single-mode OTDR's compared with multimode fibers. The prediction of the critical power levels of about 3-4 W for the onset of nonlinear effects in fibers is shown to be in good agreement with experiment. Fusion welded splices do not demonstrate significant backscattered power.**

INTRODUCTION

In all optical communications systems there is a need to examine the transmission medium, after it is installed, for fault location and for determination of the characteristics of the medium in a field environment. In the factory most of the transmission medium parameters are determined by a two-point technique since both ends of the line are accessible. In a field situation, however, it is not always practical to have access to both ends of the transmission medium. Time domain reflectometry was developed for conventional copper wire transmission systems to overcome this problem and can also be applied to optical transmission media.

Two early papers on optical time domain reflectometry (OTDR) [1], [2] outline the basic approach. A short pulse of light is launched into the fiber and the backscattered signal is monitored as a function of time (or equivalently, distance) along the fiber. The magnitude of the backscattered signal is dependent on the Rayleigh scattering, attenuation, imperfections and splices, and optical power level in the fiber. OTDR can, therefore, be used to measure attenuation and splice loss, and for fault location. For multimode fibers the attenuation and splice loss measurements are complicated by the uncertainty in the modal power distribution of the backscattered signal, as well as the variation in scattering levels of the fibers on either side of the splice. Typically, at 0.825 μm, the length of fiber that can be examined is about 5 km.

As interest shifts to longer wavelengths and single-mode fibers, the range of OTDR measurements must be increased dramatically. The lower loss of long wavelength fibers together with the high data rate of single-mode fibers make possible repeaterless spans of fiber in excess of 40 km, which must be examined during and after installation. For single-mode fibers, attenuation and splice loss measurements are potentially more reliable than in multimode fibers since the backscattered information is contained in only one propagating mode.

In this paper we present a theoretical analysis of OTDR for single-mode fibers which corrects previously published work and indicates important considerations in the design of such an OTDR measurement system. Experimental verification of the predictions of the onset of nonlinear effects are presented and a single-mode OTDR which can detect the end of 30 km of fiber with one-way loss of 1.1 dB/km is demonstrated.

Before a detailed discussion of the results of this paper, the recent rapid progress of single-mode OTDR necessitates a review of previous work.

OVERVIEW

Recently, a theoretical treatment of backscattering in single-mode fibers was presented [3], and shortly thereafter, several papers were published on experimental results of single-mode OTDR [4]-[6]. Two of the experimental papers [4], [5] used a modified avalanche photodiode (APD) operating as a photon counter and a diode laser operating at 0.85 μm. Only a single channel of the photon counter was used for signal acquisition with a fault signified by a sudden increase in the dwell time of the photon counter. Attenuation or splice loss measurements using this method were not demonstrated. A third experimental paper [6] used a Q-switched Nd:YAG laser operating at 1.06 μm as the source. A higher power laser source was necessary to overcome the additional loss penalties not found in multimode OTDR's.

One design problem with OTDR's is to couple a large amount of power into a fiber while preventing saturation of the detector with the Fresnel reflection from the fiber end face. Virtually all OTDR schemes attempt to minimize this effect. The scheme used in [6] couples the input power through a twisted multi-

Manuscript received March 15, 1982; revised May 12, 1982.
The authors are with Bell Laboratories, Norcross, GA 30071.

0018-9480/82/1000-1487$00.75

mode splitter into the single-mode fiber. The optical path is effectively index matched from the point of launch to the detector. Even though the coupling of the multimode splitter to the single-mode fiber is inefficient, enough power is still available from the Nd:YAG laser to generate Raman frequencies in the single-mode fiber. Since this is undesirable for an attenuation measurement, the input power is decreased to a point just below the onset of Raman generation. Additionally, the multimode splitter acts with unity efficiency in capturing the backscattered radiation. The next advance in single mode OTDR used a single-mode/multimode splitter [7], providing greater coupling efficiency into the single-mode fiber and a good signal-to-noise ratio over 2.1 km of fiber.

Beamsplitters have traditionally been used in multimode OTDR's, but should be used with caution for single-mode applications. Single-mode fibers are actually bimodal fibers consisting of two orthogonal polarizations of the same fundamental mode. Beamsplitters which have been coated for both "*s*" and "*p*" polarizations do not have the same splitting ratio for each polarization. Although some researchers have used beamsplitters tilted at an angle to minimize this problem, the uncertainty introduced by the use of a polarization sensitive device in a single-mode OTDR further complicates the problem, and its use should be avoided. It should be pointed out that polarization sensitive components may be used as an advantage to investigate the polarization properties of the backscattered radiation [8].

At this time, two approaches are being pursued, one directed towards single-mode OTDR over moderate distances (up to 20 km) using conventional system laser sources, and the other towards extending the OTDR range to long distances regardless of the source required. Healey [9], using the same apparatus as in [4] and [5], but with a 1.3 μm InGaAsP laser and a germanium APD detector (acting as a photon counter), demonstrated fault location over 3.4 km of single-mode fiber with a loss of 18 dB. He has extended this technique to measure attenuation and splice loss over a 20 dB range by using a multichannel analyzer [9]. Both methods use a polarization sensitive beamsplitter.

Aoyama *et al.* [10], using a polarization splitter type directional coupler with their 1.3 μm InGaAsP laser and APD, detected a fiber break at the end of 17 km of fiber. This polarization sensitive device caused problems with loss measurements, but provided good isolation from the input Fresnel reflection. The subsequent use of a polarization scrambler allowed splice and attenuation measurements out to 7 km while detecting a break at 17 km. Heckmann *et al.* [11] used fibers which were single mode at 0.82 μm with a conventional CW laser diode operating in the pulsed mode at 0.82 μm. The dynamic range was 12 dB of one-way loss, and attenuation and splice loss measurements were made over 5 km of fiber.

For long distance applications the source used is the Nd:YAG laser described in [6]. Nakazawa *et al.* [12] used an Nd:YAG operating at 1.06 μm, but employed the polarization properties of the input beam with a TeO_2 acoustooptic modulator to gate the return signal and thus block the Fresnel reflection from the detector. Splice loss and attenuation measurements were made out to 18.4 km with fault location to 19.2 km. The total dynamic range was estimated to be 50 dB. Nakazawa and Tokuda [13] extended the range by operating the Nd:YAG laser at 1.32 μm where lower loss permitted greater lengths of fiber to be measured. Using an amplifier on the Ge-APD they measured fiber attenuation for fibers with average loss of 0.63 dB/km out to 30 km, fiber break point without Fresnel reflection to 34 km, and fiber end with reflection to 40 km. The reported dynamic range was 91 dB. Additional comments on this dynamic range will appear later in this paper.

Theory

The backscattered power level $P(t)$ at the detector ($z = 0$) at time t due to scatterers a distance z ($= v_g t/2$) from the detector, can be written as[1]

$$P(t) = E(o)\, C(z)\, v_g \tag{1}$$

where v_g is the average group velocity of the fiber modes, $E(o)$ is the energy initially excited in the forward traveling pulse at $z = 0$, and $C(z)$ is the containment factor of the backscattered power, i.e., the fraction of total power lost that is captured, S, and guided back to the detector from scatterers a distance z away. In terms of the conventional scattering factor S for Rayleigh scatters

$$C(z) = S\, \alpha_R\, e^{-2\alpha_T z} \tag{2}$$

where α_R is the Rayleigh scattering component of total loss α_T. Equation (1) is a factor of 2 larger than reported in [3] and [15]. The reason for this is given in Appendix A. Apart from the varying input power coupling efficiencies of different fiber designs, the term that should be compared for relative backscattering levels of different fibers is the containment factor $C(z)$.

For multimode fibers, the backscattering factor S has been derived from a geometric optics argument and can be written as [3], [15]

$$S = \eta(2\Delta_M) \tag{3}$$

or equivalently in terms of the maximum acceptance angle of the multimode fiber $\theta_{CM}(=\sqrt{2\Delta_M})$

$$S_M = \eta\, \theta_{CM}^2 \tag{4}$$

where $\Delta_M = (n_{co} - n_{cl})/n_{co}$ is the maximum relative refractive index difference between core and cladding, and η is a function of the power distribution of the backscattered power. For uniform power distributions [3], [15]

$$\eta = \tfrac{3}{8} \text{ for step-index fibers}$$
$$= \tfrac{1}{4} \text{ for quasi-parabolic graded index fibers.} \tag{5}$$

Due to the strong wave characteristics of single-mode fibers, the geometric optics analysis for S used to derive the above equations is invalid, and the only electromagnetic analysis for single-mode fibers has offsetting errors in the execution of the

[1] We ignore for this argument the finite length of the pulse, as this only reflects in the resolution of the OTDR trace.

approach which yields the correct expression for S_S, but is a factor of 2 below the correct result for the total backscattered power. (To preserve continuity, the elucidation of the error has been given in Appendix A.) So that

$$S = \frac{3}{2}(2\Delta_S)\left(\frac{W_o V}{a}\right)^{-2}. \tag{6}$$

In terms of the diffraction angle α_D of the Gaussian beam of the fundamental mode

$$\alpha_D = \lambda/\pi n_{co} W_o \tag{7}$$

the backscattering factor S_S can be written as

$$S_S = \tfrac{3}{8}\,\alpha_D^2. \tag{8}$$

In (6) W_o is the spot size of the fundamental mode beam (i.e., e^{-2} decay of the maximum intensity in the radial direction), a is the core radius, and Δ_S is the normalized refractive index difference of the single-mode fiber. The normalized frequency of the single-mode fiber V is given by the following [14]:

$$V = 2\pi/\lambda n_{co}\, a\sqrt{2\Delta_S}\,. \tag{9}$$

The form of (8) for S_S is the most useful since it requires measurement of only one parameter of the single-mode fiber—and it also allows direct comparison with the multimode fiber result since both are now in geometric optics terminology.

In Fig. 1, we have plotted the backscattered power level $P(z)$ of (1) and (6) to a length of 40 km for particular choices of single-mode fiber parameters where the input power is 1 dB below the onset of nonlinear effects. Fig. 1 illustrates the significance of the role of the attenuation coefficient α_T, viz. for shorter wavelengths where Rayleigh scattering is higher, the initial backscattered signal is larger, but the signal decays more rapidly due to the correspondingly larger total attenuation.

To investigate the relative backscattering efficiency of single-mode fibers compared to multimode fibers, we define the backscattering efficiency factor δ_B where

$$\delta_B(z) = -10\log\left(\frac{P(z)_S}{P(z)_M}\right) \tag{10}$$

$$= \delta_E + \delta_S + \delta_A + \delta_R, \tag{11}$$

the subscripts S and M referring to the single-mode and multimode fiber, respectively.

We have separated out four independent factors affecting the relative power levels so that each independent component can be parameterized by a single variable. The total efficiency factor can then be determined for any arbitrary combination of these parameters. These four factors are defined in Table I with a range of typical values given. The component due to the different backscattering factors δ_S is plotted in Fig. 2 for the case of step-index multimode fiber as a function of the ratio of solid angles of acceptance of single-mode and multimode fibers, respectively. For parabolic index multimode fibers, the result is about 1.8 dB less of a loss penalty than the step-index fiber for all values of (α_D/θ_{CM}) due to the reduced power acceptance of the graded index multimode fiber as compared with the step-index fiber [e.g., see (4)]. The backscattering efficiency factor δ_B for any arbitrary choice of fibers lies between 10 and 18 dB.

Experiment

The experimental apparatus is essentially that described in [6] and is shown in Fig. 3. An Nd:YAG laser which operates at 1.064 or 1.319 μm was used as the source. 5 W of power were available in a CW mode at 1.064 μm and 1 W at 1.319 μm. The laser was Q-switched by the use of an acoustooptical modulator operating at 500 Hz to provide pulses of 0.7 μs duration at 1.064 μm, and 1.7 μs at 1.319 μm. The beam was launched into the fiber through a twisted, multimode, four port splitter. This has the advantage of making the optical path from the launch point to the detector appear as an index-of-refraction matched system. The extra arm of the four port splitter was immersed in index oil to eliminate unwanted reflections. The use of this multimode splitter for a single-mode fiber requires a multimode fiber to be spliced to a single-mode fiber. This results in more loss than would be incurred with a single-mode splitter spliced to a single-mode fiber. However, there are currently no single-mode/single-mode splitters commercially available that can handle the large peak powers required. Since we were able to saturate the test fiber (generate Raman shifted components) using the multimode splitter, the use of a single-mode splitter would have required more attenuation of the pump laser.

The power coupling efficiency of the splitter was determined by measuring the power launched into the splitter and then measuring the power in the single-mode fiber after 1 or 2 m. This power level was down 9 dB below the launched power. A 50/50 splitting ratio for the splitter gives a net launch penalty of 12 dB for the power received at the detector. In the case of a single-mode/single-mode splitter we would have ~9 dB penalty (3 dB in each direction for the splitter and a realistic launched power penalty of 3 dB for the single-mode fiber). Interestingly, a single-mode/single-mode splitter is only twice as efficient as a multimode/multimode one in this case.

The detector was a Texas Instruments germanium APD used without amplification. The backscattered signal received by the detector was processed by a Tektronix 7854 waveform processing oscilloscope which allowed signal averaging, storage, or transfer to a plotter. Typically, 100–1000 sweeps were averaged. The beamsplitter provides isolation from the input, but still allows some backscatter which causes the detector to overshoot the baseline. This may induce a dc offset on the baseline which has to be subtracted. A TeO_2 modulator [13] providing about 30 dB of isolation minimizes this problem, but it is susceptible to damage at the high power levels used in these studies.

Results and Discussion

The power required to generate nonlinear frequency components such as stimulated Raman scattering is known as the critical power and its formulas are presented in Appendix B. The critical power as a function of wavelength for a typical fiber used in this study is shown in Fig. 4. The critical power level is characterized by a splitting of the return pulse with the

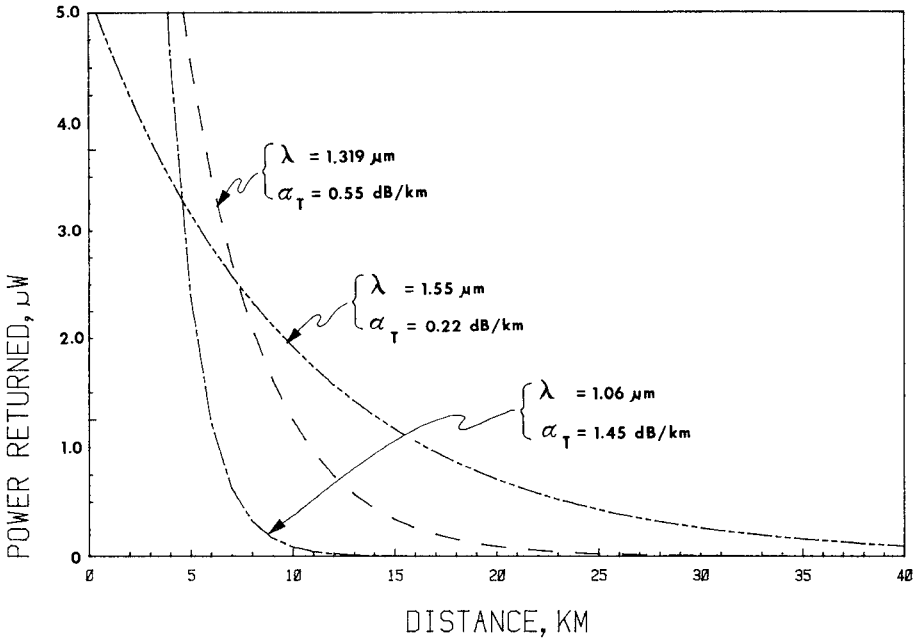

Fig. 1. Backscattered power level as a function of length for three different wavelengths.

TABLE I
COMPONENTS OF THE BACKSCATTERING EFFICIENCY FACTOR $\delta_B(z)$

Component	Formula	Typical Value
Excitation Efficiency $-\delta_E$	$-10 \log \left(\frac{E_S(o)}{E_M(o)}\right)$	3 to 8 dB
Backscattering Factor $-\delta_S$	$-20 \log \left(\frac{\alpha_D}{\theta_{CM}}\right) - 10 \log \left(\frac{3}{8n}\right)$	6 to 8 dB
Rayleigh Loss $-\delta_R$	$-10 \log \left(\frac{\alpha_{RS}}{\alpha_{RM}}\right)$	1 to 2 dB
Total Attenuation $-\delta_A$	$2z\ (\alpha_{TS} - \alpha_{TM})$	

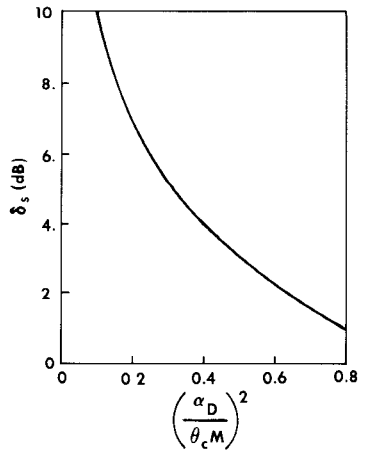

Fig. 2. The effective numerical aperture component δ_S of the relative backscattering efficiency factor δ_B, for a step-index multimode fiber. For parabolic index multimode δ_S is reduced by 1.8 dB.

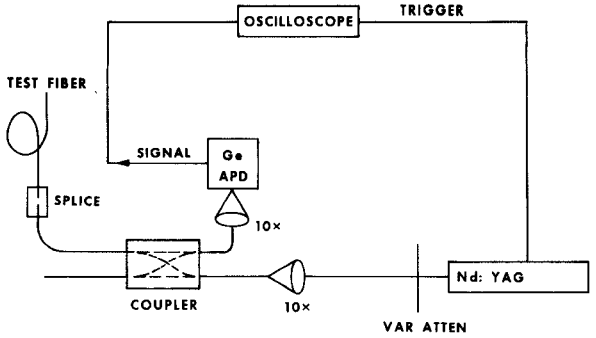

Fig. 3. Experimental apparatus used to study dual wavelength single-mode OTDR.

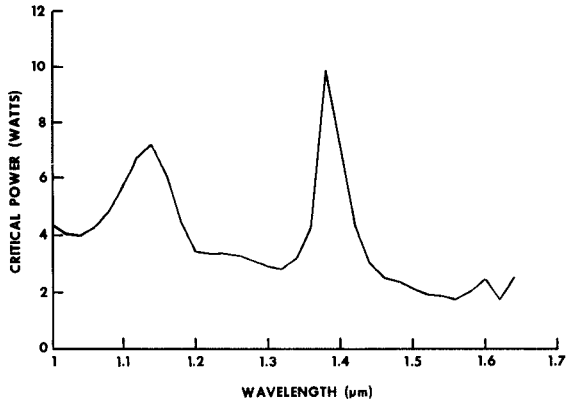

Fig. 4. Critical power, the onset of nonlinear optical effects, as a function of wavelength for a typical single-mode fiber.

Raman shifted frequencies traveling through the fiber at a different velocity than the probe pulse. Thus, they arrive at the detector at a different time from the probe pulse and the backscattered pulse appears to split. The critical power for the onset of nonlinear effects was measured for each wavelength and found to be 4.4 W at 1.064 μm and 3.6 W at 1.319 μm. This is in excellent agreement with the calculations for the critical power of 4.3 and 3.0 W for 1.064 and 1.319 μm, respectively. This power level places an upper limit on the amount of power which may be launched into the fiber and still make reliable attenuation measurements. The launched power levels used for the following OTDR measurements were approximately 1 dB below the onset of the nonlinear effects.

Two long lengths of fiber were investigated. Seven reels of different single-mode fibers were spliced together to give a length of 20.4 km with additional fibers spliced to generate a 28.5 km length. The measured one-way loss of the 20.4 km including splices was 22 dB which is an average loss of 1.08 dB/km. For the 28.5 km, the one-way loss was 31.3 dB which results in an average of 1.1 dB/km. The two-point loss measurements on the long concatenated lengths were done at 1.064 μm because of the lack of a suitable calibrated detector at 1.319 μm. The use of different fibers simulates an actual repeater span where nonidentical fibers are spliced together. Some fibers had higher V numbers (more multimode) at 1.064 μm than others, however, all of the fibers were single-mode at 1.319 μm. One particular fiber also had a smaller core diameter and a different index profile shape than the others. Some of the splices were V-groove index-matched splices and some were fusion welded. The typical individual fiber length was about 2.5 km.

The single-mode OTDR plot of the 20.4 km at 1.319 μm is shown in Fig. 5(a). The splices are labeled according to type, with the V-groove labeled (V) and the fusion welded labeled (F). The fiber located between splice $V2$ and $V3$ has a smaller core, and its profile shape is significantly different from the other fibers. This is evidenced by the large reflected spike at $V3$. Fig. 5(b) shows the 1.064 μm OTDR plot of the same 20.4 km. Comparing Fig. 5(a) and (b), one observes that the magnitude of the reflection spike from the V-groove splices is strongly dependent on the wavelength and the quality or loss of a particular splice cannot be inferred from the magnitude of this reflection. The attenuation of a particular fiber section is clearly discernable in the 1.319 μm plot, and attenuation measurements were possible on all of the fiber sections up to 18.7 km. The fiber between $V2$ and $V3$ was measured by OTDR to be 0.7 dB/km and the fiber between $F1$ and $V5$ to be 0.86 dB/km. The separate fibers were measured previously by a two-point technique to have losses of 0.8 and 0.82 dB/km, respectively. The other fibers in this 18.7 km section showed similar agreement with previous measurements. The last fiber section ($V5$ to 20.4 km) was shorter than any of the other fiber lengths and the combination of short length and lower signal to noise at that distance increased the uncertainty in the attenuation measurement for that section. Hence, reliable attenuation measurements were only made to 18.7 km.

The shape of these plots is qualitatively in agreement with the wavelength dependence of the backscattered power calculations of (1) and Fig. 1. That is, while there is initially more backscattered power at 1.064 μm, it is quickly attenuated, and the backscatter at 1.319 μm is initially lower, but does not decay as rapidly. The differences in the reflection spikes of the splices for the plots at the two wavelengths may be because the fibers are not single mode at 1.064 μm. The significant differences in attenuation and splice loss (for instance, $V1$) make it imperative that the wavelength used for the OTDR be the same as that used for the system application. In comparing these two plots, one would not *a priori* conclude that they were measured on the same identical fiber span.

An additional length of 8.1 km of fiber was fusion welded onto the existing 20.4 of Fig. 5, and these OTDR plots, Fig. 6(a) and (b), compare the decay at 1.319 μm to that at 1.064 μm. Comparing Figs. 5(a) and 6(a), we note the good agreement for the first 20.4 km in which all fibers of the spans were single moded. However, Figs. 5(b) and 6(b) demonstrate large differences in the reflection spikes from splices. Because the fibers are multimode at that wavelength, the input modal power distribution is sensitive to launch conditions. In the case of the 1.319 μm plot, Fig. 6(a), only the reflection from the fiber with the different profile and V-groove splice is clearly evident, however, at 1.064 μm the first four of the V-groove splices are quite obvious. Using the measured loss at 1.064 μm by the two-point technique, the end of the fiber was detected after a roundtrip loss of 63 dB. For lower loss fibers, this would mean we could detect ends much farther than 28.5 km. For a fiber loss of 0.6 dB/km, this roundtrip loss translates to more than 50 km for end detection.

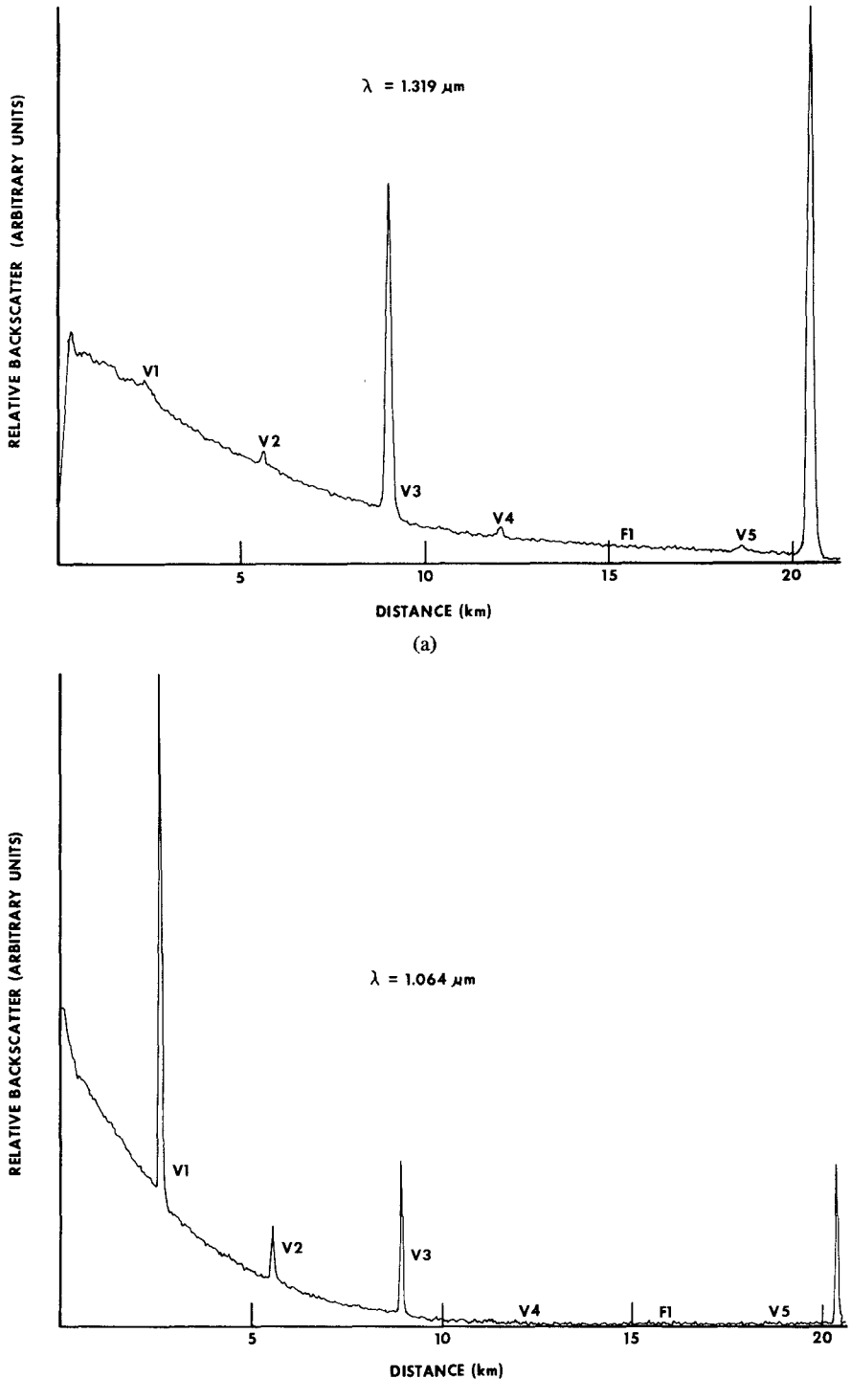

Fig. 5. Single-mode backscatter plot of 20.4 km of fiber showing the different attenuation and range characteristics for (a) 1.319 μm and (b) 1.064 μm.

It is customary for researchers to use the term dynamic range as a "figure of merit" for their OTDR's, and many papers have appeared in the literature quoting a certain dynamic range. However, the numbers reported should be interpreted with caution. For a full description of the capabilities of an OTDR, three separate dynamic ranges are necessary: 1) the range in dB over which detection of a reflecting break is possible; 2) the range in dB for locating a nonreflecting break; and 3) the range in dB over which attenuation and splice loss can accurately be determined. In most instances the range for 2) and 3) should be similar.

A critical factor in determining the dynamic range of attenuation and splice loss is an accurate evaluation of the baseline of the system, that is, the dc level of the random noise of a homogeneous medium. Improving the precision of this baseline determination can greatly increase the dynamic range.

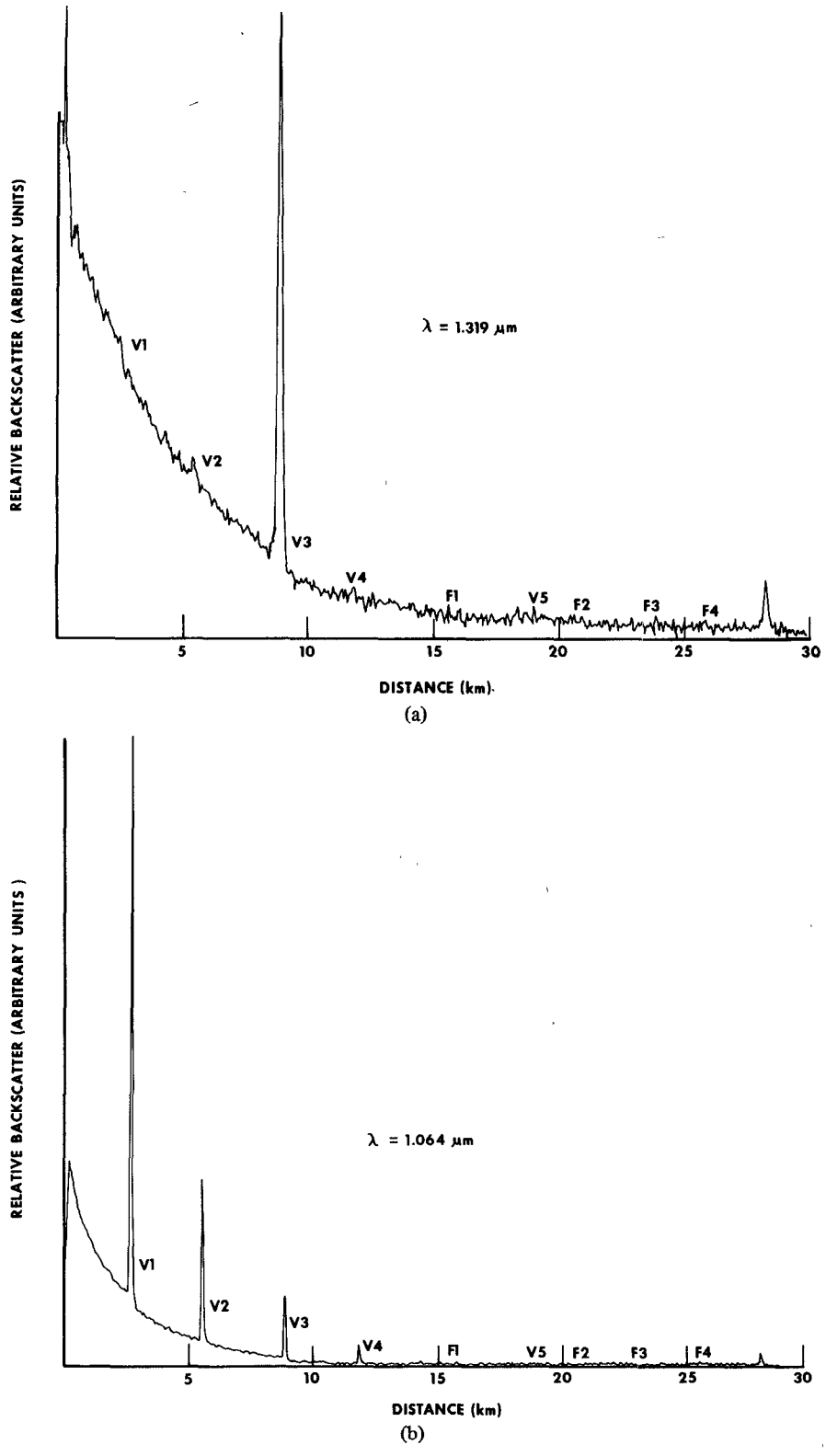

Fig. 6. Single-mode backscatter plot of 28.5 km of fiber showing the extended range capabilities of (a) 1.319 μm versus (b) 1.064 μm.

When one considers long continuous lengths of fiber that are relatively uniform, the dynamic range over which loss measurements can be made is greater than for short lengths, due to the statistical averaging of the backscattered signal, as indicated previously in the discussion of Fig. 5. Thus, for loss measurements, the most pessimistic dynamic range, but the most useful for diagnosis, is the ability to determine local attenuation. These statements obviously also hold for splice loss evaluation. By these three quoted dynamic ranges for an OTDR and the average loss for the fiber, one can determine the lengths over

which reliable measurements can be made. That is, the measurable length in km equals the dynamic range in dB divided by the average attenuation in dB/km.

The results of [13] represent the present state of the art for single-mode OTDR with end detection to 40 km, nonreflecting fault location to 34 km, and attenuation and splice loss to 30 km of fiber with average loss of 0.63 dB/km. Using the above definition of dynamic range, these length measurements indicate that the OTDR of [13] has dynamic ranges of 50, 43, and 38 dB for end detection, nonreflecting fault location, and attenuation and splice loss, respectively. However, the fiber used in this measurement appears to be one continuous 40 km length with no splices present. Various authors [12] report a single dynamic range which in some instances includes effects which do not translate to the length measurement capability of the above definition. The reported dynamic range of 91 dB of [13] probably includes these effects.

Finally, Fig. 7 is an OTDR trace of the 28.5 km of spliced fiber from the opposite end and shows the effect of a fusion splice. The V-groove splices used in this study all showed some reflection, probably because of an improper index match between the index matching material and the fiber. Fig. 7 indicates that in fusion splices there is no reflected spike even for poor quality (high loss) splices. Backscattering from splices can affect the output characteristics of diode lasers [16] and it is important to determine if such a reflection exists. The fusion splice was intentionally made to have high loss to investigate this potential problem, and Fig. 7 indicates that this effect is not important for fusion splices even when the splice loss is as large as 0.95 dB, as in Fig. 7. The absence of a reflected spike is thought to occur because there is a blending of the material in the fusion process which reduces any index discontinuity.

Conclusions

We have demonstrated the ability to examine long lengths of single-mode fiber in excess of 60 dB of two-way loss. Using fibers with lower attenuations, fault location and end detection could be achieved for lengths of fiber greater than the 28.5 km studied here. Using the nonlinear effects, end detection of 54 km has been reported in the literature [17]. With the end detection definition of the dynamic range of the system, the technique presented has a 63 dB range. The theory presented here allows one to determine the expected loss penalty in using OTDR for a single-mode fiber in comparison to an arbitrary multimode fiber. Furthermore, we observe that for long lengths of single-mode fiber the loss penalty can be a function of length due to the attenuation differences between single-mode and multimode fibers. The measured and calculated critical powers for the onset of nonlinear effects are in excellent agreement. This is very important since it places an upper limit on the power available for attenuation measurements.

From the OTDR results we see that is is imperative to measure the fiber at the anticipated operating wavelength because the splice loss and the reflection spikes of the splices change considerably with wavelength. It is obvious that the splice loss should be measured at the system operating wavelength because the spot size of the fundamental mode (which determines the magnitude of the splice loss) changes significantly with wavelength. The large reflection spikes from the V-groove splices are not well understood and further study is necessary. However, it is important to note that the quality of the splice (loss) cannot be determined from the magnitude of the reflection spike. The fused splices do not demonstrate any back reflection as the fusing of the glass creates a situation which favors forward scattering.

The recent experimental work [22] that shows excellent agreement with the results of [3] for the backscattering factor S_S, does not conflict with the analysis presented here, due to the large uncertainties in the fiber parameters (particularly α_S) and measurement techniques. Furthermore, it must be remembered that [3] (and this paper) assumes that the only mechanism for backscattering is Rayleigh scattering.

Appendix A

As indicated in [15], the length of fiber at point z that contributes to the power received at time t ($= 2z/v_g$) by the detector at $z = 0$ is only half the full input pulse width, i.e., $l_{p/2}$ (the spatial pulse width is $l_p = v_g \tau$, where τ is the temporal width). However, every elemental segment dz of the input pulse scatters power from some section dz of this length ($l_{p/2}$) that contributes to the power received at the detector at time t. This results in an effective length of scatters of l_p, NOT $l_{p/2}$ as stated in [15] and implicitly assumed in [3], since each elemental length dz of the scattering region cannot be uniquely associated with one elemental segment dz of the input pulse (for the power arriving at the detector at time t). Thus, the total backscattered power at time t from the region is equal to the power scattered from a length equal to the full pulse width l_p. This results in (1).

To completely define the backscattered power we need to have expressions for S'—the backscattering factor. If we consider that only Rayleigh scatterers contribute to the backscattered power, then

$$S' = S\,\alpha_R/\alpha_T$$

where S is the backscattering factor for Rayleigh scattering and α_R/α_T is the relative amount of total power lost due to Rayleigh scattering. For multimode fibers, the Rayleigh component of S' has been evaluated correctly in [15] via a geometric optics analysis. For single-mode fibers the only electromagnetic analysis of S in the literature is beset by errors [some of which are offsetting, e.g., the two errors incurred in going from (9)–(11)] but yields the correct expression for S. Due to the above-mentioned error in the general formula, the backscattered power is a factor of $\frac{1}{2}$ of the correct result. For a more complete and correct derivation of S_S see [23].

Appendix B

The input power can be increased only up to a threshold value beyond which nonlinear effects become important. The nonlinear phenomena of most concern are stimulated Raman scattering (SRS) (forward and backward interaction), and stimulated Brillouin scattering (SBS) (backward interaction). Both phenomena cause power to be transferred to other frequencies that propagate at different velocities and subsequently degrade the return signal. This threshold power is

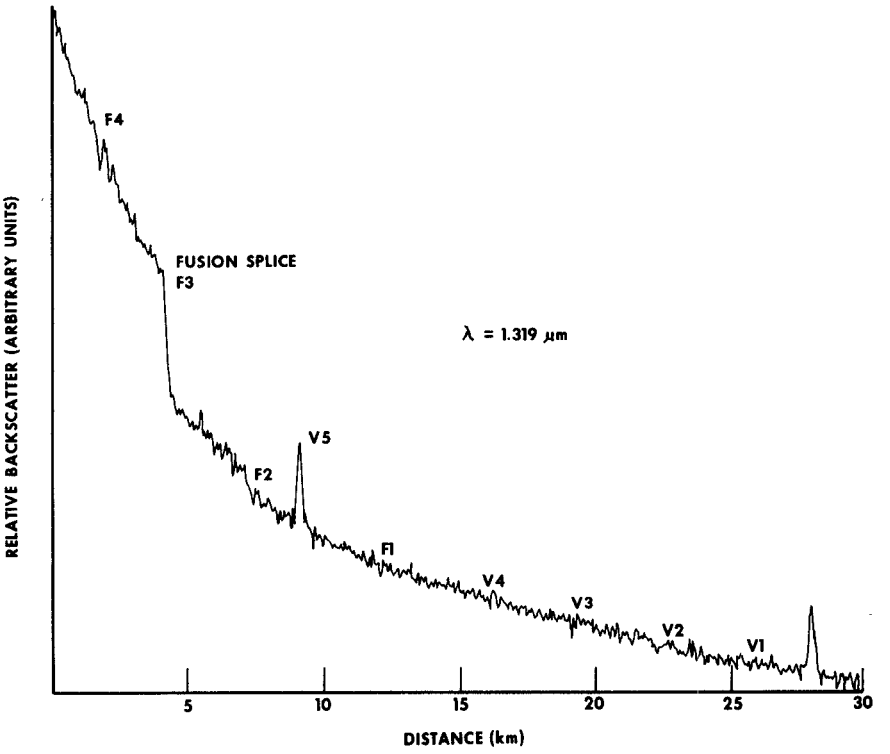

Fig. 7. A high loss fusion splice showing the absence of a reflection spike characteristic of other types of splices.

dependent on spectral loss and Raman and Brillouin scattering efficiency.

Calculation of Critical Powers

Approximate expressions for critical input power have been derived by Smith [18]. The derivation requires that the power in the stimulated wave be everywhere less than the input wave power. Operating 1 dB down from the critical value will reduce the stimulated wave by 20 dB and assure an adequate safety margin [18]. The critical power for SRS, forward interaction (i.e., the SRS wave propagates in the forward direction) is

$$P_{\text{crit}} = \frac{16\, A_{\text{eff}}}{L_{\text{eff}}\, g_o}. \tag{B1}$$

For pulses such as those used in the OTDR, P_{crit} represents peak power. A_{eff} is an effective core area related to the amount of overlap between the pump mode and the Stokes mode. If there is little overlap between the modes, there will be fewer photons available to supply the stimulated process, and the critical power will be correspondingly greater. A_{eff} varies inversely with the V number and ranges from 0.94 times the core area for $\lambda = 1.0$ μm ($V = 3.01$) to 1.7 times the core area for $\lambda = 1.64$ μm ($V = 1.83$) [19]. Here, V is defined as in (6) of the text. L_{eff} in (B1) is an effective length given by [20]

$$L_{\text{eff}} = \frac{1 - e^{-\alpha l}}{\alpha} \tag{B2}$$

where αl is the total attenuation in nepers. For long lengths of fiber where material dispersion is sufficiently small, L_{eff} is approximately equal to $1/\alpha$. The Raman gain coefficient g_o equals 0.5×10^{-11} cm/W for fused silica at 1.0 μm when polarization is not maintained and scales [21] as $1/\lambda$.

Fig. 4 is a plot of critical power as defined in (B1) versus wavelength. The spectral loss data from a typical single-mode fiber were used to calculate L_{eff}.

The expression for critical power for backward SRS is

$$P_{\text{crit}} = \frac{20\, A_{\text{eff}}}{L'_{\text{eff}}\, g_o} \tag{B3}$$

where A_{eff} and g_o are as defined previously and L'_{eff} is half the length of the pump (input) pulse in the fiber. Since $L'_{\text{eff}} \ll L_{\text{eff}}$, the critical power for backward SRS is greater than P_{crit} for forward SRS, and it will not be a limiting factor.

P_{crit} for SBS is given by the following:

$$P_{\text{crit}} = \frac{21\, A_{\text{eff}}}{L'_{\text{eff}}\, G} \tag{B4}$$

where again L'_{eff} is half the length of the pump pulse in the fiber and G, the gain coefficient, is [21]

$$G = \frac{8.65 \times 10^{-11}}{\lambda^2\, \Delta\nu_p} = \text{cm/W} \tag{B5}$$

where it is assumed that polarization is not maintained and $\Delta\nu_p \gg \Delta\nu_\beta$, where $\Delta\nu_p$ is the spectral width of the pump in GHz (full width-half maximum) and $\Delta\nu_\beta$ is the linewidth of the Brillouin scattering. Comparing (B4) and (B5) with (B1) it is easily seen that

$$\frac{P_{\text{crit}}\ (\text{SBS})}{P_{\text{crit}}\ (\text{SRS})} \simeq 6.03\, \lambda\, \frac{L_{\text{eff}}}{L'_{\text{eff}}} \tag{B6}$$

for λ in μm, and $\Delta\nu_p \simeq 80$ GHz. Typically, L_{eff} will be at least two orders of magnitude greater than L'_{eff}; hence, forward SRS will set the upper limit on input power.

REFERENCES

[1] S. D. Personick, "Photon probe–An optical-fiber time-domain reflectometer," *Bell Syst. Tech. J.*, vol. 56, pp. 355-366, 1979.

[2] M. K. Barnoski, M. D. Rourke, S. M. Jensen, and R. T. Melville, "Optical time domain reflectometer," *Appl. Opt.*, vol. 16, pp. 2375-2379, 1977.

[3] E. Brinkmeyer, "Analysis of the backscattering method for single-mode optical fibers," *J. Opt. Soc. Amer.*, vol. 70, pp. 1010-1012, 1980.

[4] P. Healey, "Optical time domain reflectometry by photon counting," in *Proc. 6th European Conf. on Opt. Commun.*, York, England, 1980, pp. 156-159.

[5] P. Healey and P. Hensel, "Optical time domain reflectometry by photon counting," in *Symp. on Opt. Fiber Measurements*, NBS Spec. Publ. 597, 1980, pp. 85-88.

[6] D. L. Philen, "Optical time domain reflectometry on single mode fibers using a *Q*-switched Nd:YAG laser," in *Symp. on Opt. Fiber Measurements*, NBS Spec. Publ. 597, 1980, pp. 97-100.

[7] B. S. Kawasaki, K. O. Hill, and D. C. Johnson, "Optical time domain reflectometer for single mode fibers at selectable wavelengths," *Appl. Phys. Lett.*, vol. 38, pp. 740-742, 1981.

[8] M. Nakazawa, T. Horiguchi, M. Tokuda, and N. Uchida, "Measurement and analysis of polarization properties of backward Rayleigh scattering for single-mode optical fibers," *IEEE J. Quantum Electron.*, vol. QE-17, pp. 2326-2334, Dec. 1981.

[9] P. Healey, "OTDR in monomode fibers at 1.3 μm using a semiconductor laser," *Electron. Lett.*, vol. 17, pp. 62-64, 1981; and P. Healey, "Multimode photon-counting backscatter measurements on monomode fibre," *Electron. Lett.*, vol. 17, pp. 751-752, 1981.

[10] K. Aoyama, K. Nakazawa, and T. Itoh, "Optical time domain reflectometry in a single-mode fiber," *IEEE J. Quantum Electron.*, vol. QE-17, pp. 862-868, June 1981.

[11] S. Heckmann, E. Brinkmeyer, and J. Streckert, "Long-range backscattering experiments in single-mode fibers," *Opt. Lett.*, vol. 6, pp. 634-635, 1981.

[12] M. Nakazawa, T. Tanifuji, M. Tokuda, and N. Uchida, "Photon probe fault locator for single-mode optical fiber using an acousto-optical light detector," *IEEE J. Quantum Electron.*, vol. QE-17, pp. 1264-1269, July 1981.

[13] M. Nakazawa, M. Tokuda, K. Washio, and Y. Morishige, "Marked extension of diagnosis length in optical time domain reflectometry using 1.32 YAG laser," *Electron. Lett.*, vol. 17, pp. 783-784, 1981.

[14] D. Marcuse, "Gaussian approximation of the fundamental modes of graded index fibers," *J. Opt. Soc. Amer.*, vol. 68, pp. 103-109, 1978.

[15] E. G. Neumann, "Theory of backscattering method for testing optical fiber cables," *Electron. Commun.*, vol. 34, pp. 157-160, 1980.

[16] Y. C. Chen, "Noise characteristics of semiconductor laser diodes coupled to short optical fibers," *Appl. Phys. Lett.*, vol. 37, pp. 587-589, 1980.

[17] K. Nogushi, Y. Murakami, K. Yamashita, and F. Ashiya, "52 km-long single mode optical fibre fault location using the stimulated Raman scattering effect," *Electron. Lett.*, vol. 18, pp. 41-42, 1982.

[18] R. G. Smith, "Optical power handling capacity of low loss optical fibers as determined by stimulated Raman and Brillouin scattering," *Appl. Opt.*, vol. 11, pp. 2489-2494, 1972.

[19] R. H. Stolen, "Nonlinear properties of optical fibers," in *Optical Fiber Telecommunications*, S. E. Miller and A. G. Chynoweth, Eds. New York: Academic, 1979, pp. 129-130.

[20] E. P. Ippen, "Nonlinear effects in optical fibers," in *Laser Applications to Optics and Spectroscopy*, S. F. Jacobs, M. O. Scully, and M. Sargent, Eds. Reading: Addison-Wesley, 1975, p. 213.

[21] R. H. Stolen, "Nonlinearity in fiber transmission," *Proc. IEEE*, vol. 68, pp. 1232-1236, 1980.

[22] M. P. Gold and A. H. Hartog, "Measurement of backscatter factor in single mode fibers," *Electron. Lett.*, vol. 17, pp. 965-966, 1981.

[23] I. A. White, "Theory of backscattering in optical fibers," submitted to *Electron. Lett.*

Dan L. Philen received the B.S. degree in chemistry from Auburn University, Auburn, AL, in 1968, and the Ph.D. degree in physical chemistry from Texas A&M University, College Station, in 1975.

From 1976 to 1979 he was with the Georgia Institute of Technology, Atlanta. Since 1979 he has been with Bell Laboratories, Norcross, GA, where he has been engaged in exploratory measurements on optical fiber properties.

Dr. Philen is a member of the American Chemical Society, the Optical Society of America, Sigma Xi, Sigma Pi Sigma, and Phi Lambda Upsilon.

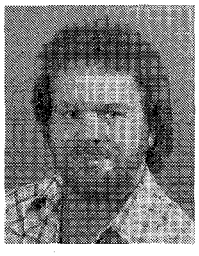

Ian A. White received the B.Sc. degree in physics from the University of Queensland, Australia, in 1974, and the Ph.D. degree in applied mathematics from Australia National University in 1977.

From 1977 to 1979 he was with the Optical Sciences Center, University of Arizona, Tucson. Since 1979 he has been with Bell Laboratories, Norcross, GA, where he is a member of the Exploratory Components and Media Studies Group.

Jane F. Kuhl received the B.S. degree in physics in 1980 and M.S. degree in electrical engineering in 1982, both from the Georgia Institute of Technology, Atlanta.

Since 1981 she has been with Bell Laboratories, Norcross, GA, where her present work involves research on optical fiber components and splicing.

Ms. Kuhl is a member of the Optical Society of America.

Stephen C. Mettler received the B.S. degree in 1962 from the United States Air Force Academy, Colorado Springs, CO, the M.S. degree in physics in 1972, and the Ph.D. degree in 1976 from Purdue University, Lafayette, IN.

Since 1976 he has been with Bell Laboratories, Norcross, GA, where he is currently engaged in research on optical fiber components and splicing.

Dr. Mettler is a member of the Optical Society of America.